

Microscale modeling of effects of realistic surface heat fluxes on pollutant distribution within a simplified urban configuration

J L Santiago¹, B Sanchez^{1,2}, A Martilli¹

¹ Air Pollution Division, Environmental Department, CIEMAT, Madrid, Spain, e-mail addresses:

jl.santiago@ciemat.es ; beatriz.sanchez@externos.ciemat.es ; alberto.martilli@ciemat.es

² Ingeniería y Economía del Transporte (INECO). Avda. Partenón 4-6, 28042 Madrid, Spain

dated : 15 June 2015

1. Introduction

Modelling micrometeorology and pollutant dispersion within urban areas is very important for both urban climate and air quality applications. The interaction between atmosphere and urban surfaces induces complex flow fields and large heterogeneities in temperature and pollutant distribution within urban canopy layer. These surface-atmosphere interactions may be classified as mechanical (blocking and deviation of the wind by obstacles) and thermal (buoyancy effects due to heat exchange between the atmosphere and buildings). Urban surface heat fluxes are responsible for temperature distribution within street inducing, in some scenarios, modifications of flow properties respect to a neutral case that can affect to pollutant dispersion. Thermal processes are usually neglected, or modeled in a simple way (one facet with different (but constant) temperature with respect to the other urban surfaces) in computational fluid dynamic (CFD) simulations. The main objective of this work is to analyse the effects of realistic surface thermal forcing on pollutant dispersion within a simple urban configuration. CFD-RANS simulations are carried out over a periodic array of cubes with a packing density of 0.25 using realistic surface heat fluxes as boundaries conditions at street and building walls. The microscale heat flux distributions are computed by the TUF3D model (Krayenhoff and Voogt, 2007). Forty four scenarios with different solar position and ratios of buoyancy to dynamical forces are simulated (Santiago et al., 2014). In this work, one passive tracer is emitted for each scenario at the bottom part of the domain representing traffic emissions. The main objective it to determine the impact of “realistic” distribution of urban surface heat fluxes on airflow properties and pollutant concentration. Concentration maps within street and the changes with respect to neutral case are analyzed. In addition, spatial average concentrations are also studied and related with properties of the flow. These results are focused on providing useful information to parameterize processes by urban canopy models. These processes are resolved by CFD but are subgrid scale with respect to typical mesoscale model grid resolutions.

2. Description of configuration and numerical set-up

The geometrical configuration studied is an aligned array of cubes with a packing density of $\lambda_f = \lambda_p = 0.25$. Figure 1 shows a scheme of the numerical domain, mesh and emission locations of the RANS simulations. The array is aligned with the cardinal directions and the flow is imposed in the x-direction. In order to simulate an infinite array, periodic boundary conditions are imposed at four lateral boundaries of the numerical domain. Flow is maintained by a downward flux of momentum ρu_r^2 imposed at the top of domain in the x-momentum equation, where ρ is air density and u_r is the friction velocity. The height of the domain is $4h$ (where h is cube height). The simulations are based on Reynolds-averaged Navier-Stokes (RANS) equations and the standard k - ϵ turbulence model. Thermal effects are considered by imposing realistic distributions of heat fluxes as boundary conditions at building and street surfaces and buoyancy terms are accounted for with Boussinesq's approximation and an equation for temperature is solved. Seven solar positions are analysed. One scenario for a 0° solar zenith angle, and two cases (one shading the windward wall and the other the leeward wall) for 60° , 45° , 30° . Figure 2 shows an example of two solar positions for a 30° zenith angle. In addition, for each solar position several ratios between buoyant and inertial forces are simulated, and a neutral case (surface heat fluxes are neglected) is also simulated. At the top, a T_{ref} is fixed allowing a flux upward out of the domain equal to $k_{eff} (T_{ref} - T) / \Delta z$ where k_{eff} is the eddy conductivity for heat at the top of the domain, and Δz is the vertical mesh size of the top cells. A cartesian grid is used which resolves each cube with 16 cells in each direction. A test of grid independence was made using 32 cells to resolve each cube (i.e., doubling the number of cells in each direction) for the evaluation case (see Sect. 3.1) and demonstrates that a resolution of 16 is acceptable. Pollutants are modelled as passive tracers. The emissions are located close to ground (Figure 1).

The methodology is the following:

- 1) Heat flux distribution due to solar position is computed by an urban energy balance model (TUF3D model, Krayenhoff and Voogt, 2007). This model is a dry, three-dimensional microscale urban energy balance model with a focus on radiative exchange. Plane parallel facets (roofs, walls, streets) are split into identical square patches, each of which exchanges shortwave and longwave radiation and sensible heat, and

store/release conduction heat.

- 2) The flow, temperature and pollutant dispersion around the buildings are simulated by a computational fluid dynamics (CFD) model (STARCCM+ from CD-Adapco) using as boundary conditions the heat fluxes computed by TUF3D model.

The ratio between buoyancy and inertial forces of the cases studied are characterized in terms of h/L_{urb} , where h is the height of the cubes and L_{urb} is an urban length scale defined analogously to the Monin-Obukhov length as,

$$L_{urb} = \frac{u_\tau^3}{\left(\frac{g}{T_{ref}} \frac{Q_h}{\rho C_p} \right)}$$

where Q_h is the total heat from all urban surfaces, divided by the plan area ($W m^{-2}$), ρ is the density of air and C_p is the specific heat of air. Cases with h/L_{urb} values from 0 to 3 are simulated. $h/L_{urb} = 0$ corresponds to the neutral case, and the higher the h/L_{urb} , the higher the buoyancy forces with respect to inertial forces. All values of h/L_{urb} are realistic. More details about configurations can be found in Santiago et al. (2014).

Velocity is normalized by u_τ , temperature differences are normalized by $\frac{Q_h / \rho C_p}{u_\tau}$ and concentration (C_{norm}) is defined as $C_{norm} = C u_\tau h^2 / Q_c$, where Q_c is the total emission per unit time.

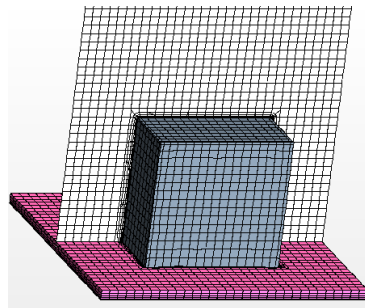


Fig. 1. Numerical domain, mesh and emission locations (in red)

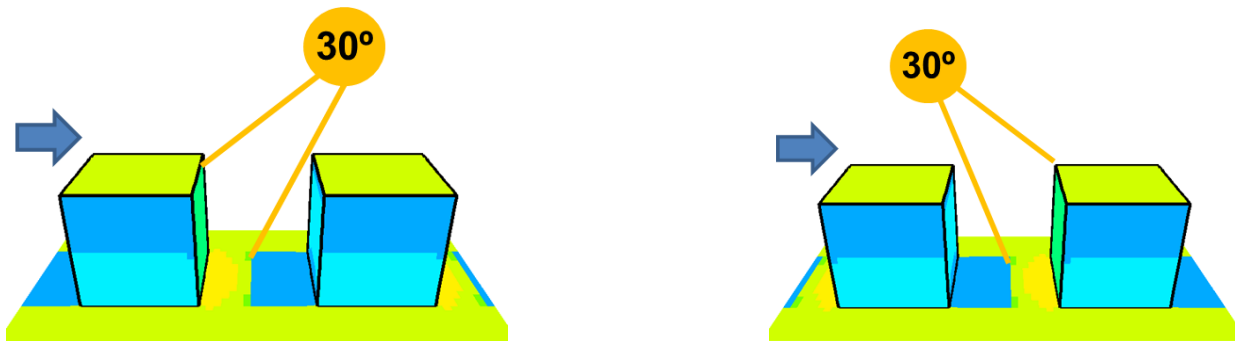


Fig. 2 Two solar positions for a 30° zenith angle

3. Microscale results

The main aim is to analyze the influence of solar position and intensity of thermal forcing (with respect to inertial forces) on the flow and normalized concentrations fields. As an example, cases with solar zenith angle of 30° heating different walls and different h/L_{urb} (intensities of thermal forcing) are analyzed. Figure 3 shows the flow field and normalized concentration for neutral case and figures 4-5 show the flow and normalized concentration for $h/L_{urb} = 0.4$, and 2.25 for the two cases with a zenith angle of 30°.

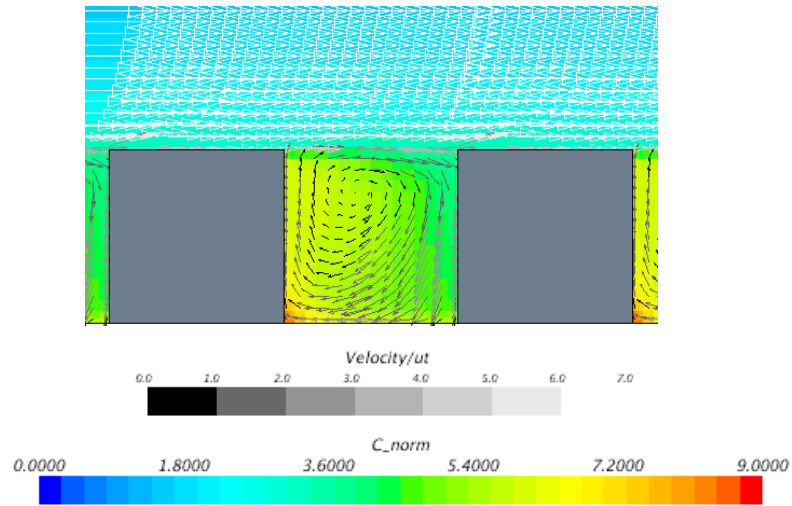


Fig. 3 Flow field and concentration for neutral

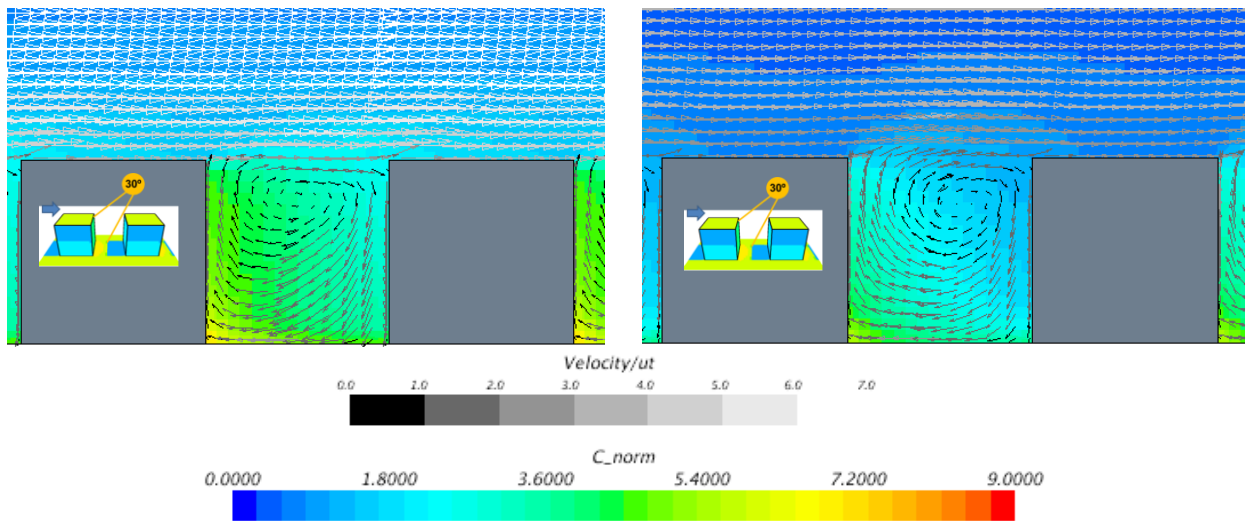


Fig. 4 Flow field and concentration for 30° leeward wall heated (Left: $h/L_{urb} = 0.4$; Right: $h/L_{urb} = 2.25$)

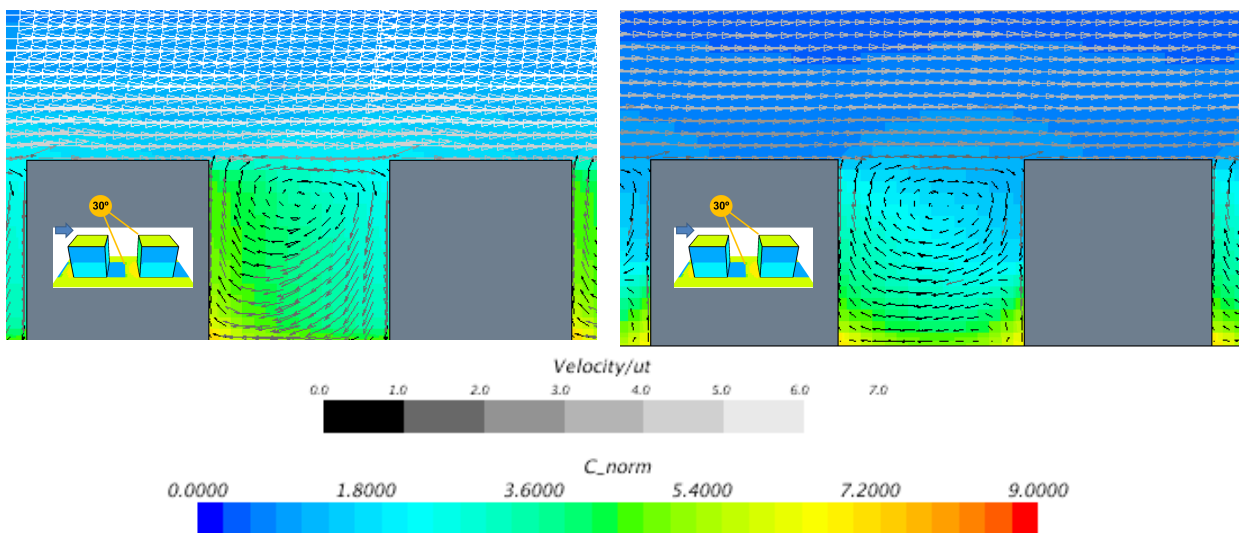


Fig. 5 Flow field and concentration for 30° windward wall heated (Left: $h/L_{urb} = 0.4$; Right: $h/L_{urb} = 2.25$)

Respect to neutral case, in general, the concentration within the canopy decreases for non-neutral cases. The higher is h/L_{urb} (intensities of thermal forcing), the lower is the concentration. This fact is because of the increase of mixing induced by surface heat fluxes. For $h/L_{urb} = 0.4$, the influence of the position of the sun (zenith angle = 30°) is negligible in the flow pattern and in the pollutant distribution within the canopy. When h/L_{urb} increases ($h/L_{urb} = 2.25$), flow patterns within the street changes from neutral case and they also show a dependency with the wall heated. If the windward wall is heated (Fig. 5), buoyancy forces at the windward wall oppose the flow. In this case, at the bottom of this wall these forces are significant, and a secondary vortex appears. This creates higher concentration and a local maximum at this wall that it does not exist for the case where the leeward wall is heated (Fig. 4). Therefore, for larger intensities of thermal forcing the pollutant distribution at microscale is sensitive to the position of the sun.

4. Spatially-averaged properties

Mesoscale models can simulate domains that cover the whole city and its surroundings but with their spatial resolution (several hundreds of meters) it is not possible to solve the flow around the buildings. Usually, urban canopy models (compromise between simplicity and accuracy) are used to parameterize processes at smaller scale than mesoscale resolution (i.e. parametrization of drag forces induced by buildings). In this way, spatially-averaged properties computed from CFD results are useful in order to provide this information to urban canopy parametrization.

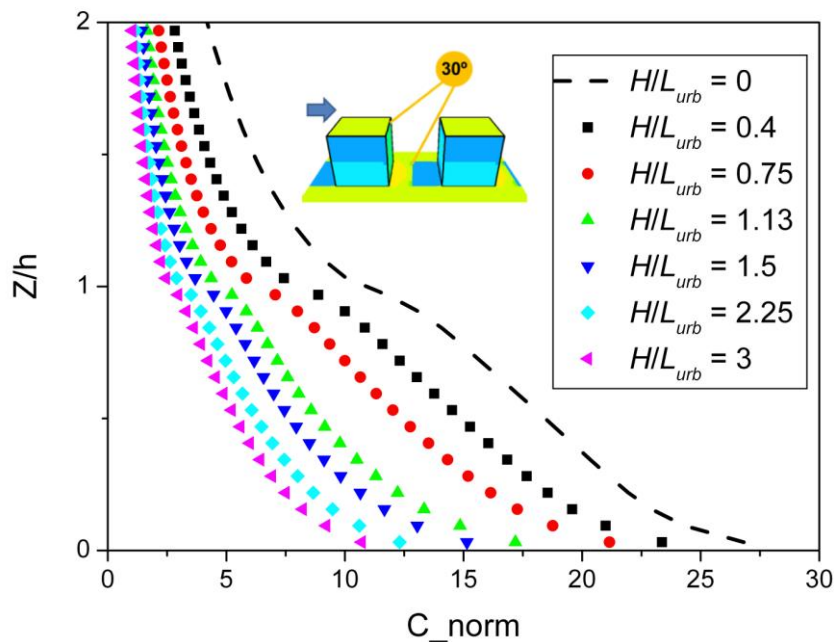


Fig. 6 Spatially-averaged profiles of normalized concentration for 30° solar zenith angle with leeward wall heated and different h/L_{urb} .

Santiago et al. (2014) analyzed the spatially-averaged wind speed and temperature. This work is focused on concentration. Figure 6 and 7 show the variation of spatially-averaged profiles of normalized concentration with h/L_{urb} for the two cases of 30° solar zenith angle. In general, the higher is h/L_{urb} , lower is the concentration.

Santiago et al. (2014) found that the spatially-averaged profiles are more dependent of the ratio between buoyant and inertial forces (h/L_{urb}) than the distribution of surface heat fluxes. For average concentration similar behavior is observed for low values of h/L_{urb} . However, in the cases of $h/L_{urb} > 1$, we found differences between the case where the windward wall is heated by the sun and the case where the wall heated is the leeward one. This fact, as explained previously, is due to the fact that buoyancy forces at the windward wall oppose the flow and reduce the ventilation of the canyon affecting not only the microscale distribution of pollutants but also the average profiles. In order to analyze the concentration average at pedestrian level, in figure 8, the ratio between average concentrations at 2.5 m for non-neutral cases divided by this concentration for the neutral case is presented. It is observed that the average concentration is reduced more than 40% for $h/L_{urb} > 1$. In addition, for the same h/L_{urb} , when this ratio is higher than 1, there are differences of 5 % in concentration for different distributions of heat fluxes. This is related with the changes of flow induced by the increase of h/L_{urb} .

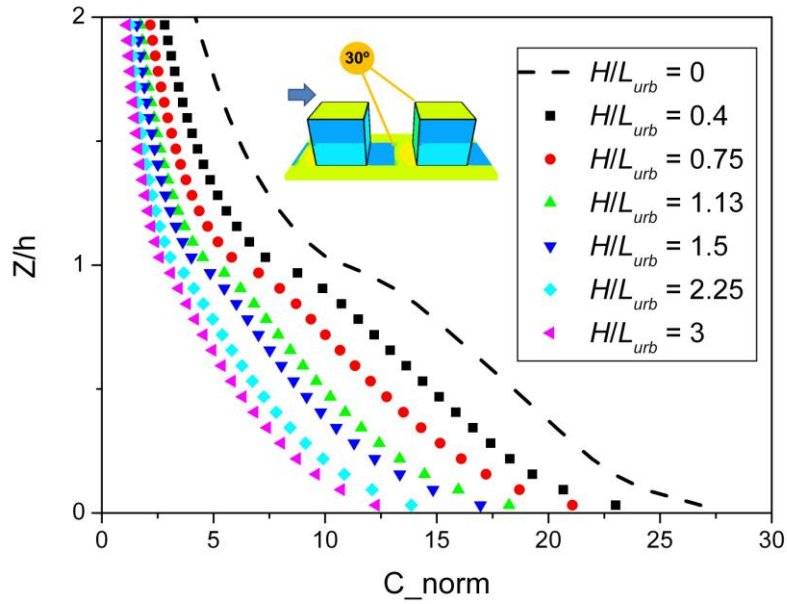


Fig. 7 Spatially-averaged profiles of normalized concentration for 30° solar zenith angle with windward wall heated and different h/L_{urb} .

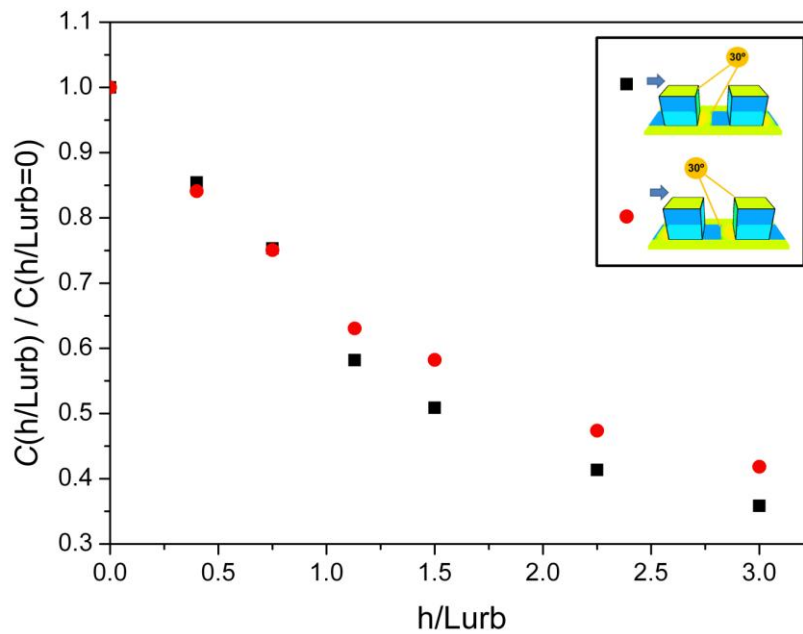


Fig. 8. Variation of spatial average concentration at 2.5 m with h/L_{urb} for the two cases of 30° solar zenith angle.

5. Conclusions

This study analyzes the effects of realistic surface thermal forcing on pollutant dispersion within a simple urban configuration. The increase of buoyant forces respect to inertial ones induces a reduction of concentration within the canopy. For $h/L_{urb} > 1$, the buoyant forces change the flow pattern and consequently vary the distribution of pollutants. Locally, at certain position close to the ground the concentration can increase. In terms of spatially-average concentration, it decreases as h/L_{urb} increases. In addition, for $h/L_{urb} > 1$, differences between the case where the windward wall is heated by the sun and the case where the wall heated is the leeward one are observed. The modification of the flow patterns induced by the increase h/L_{urb} has influence in the spatially average properties as C_d and average concentration.

Acknowledgment

This study has been partially supported by the project Modelización de la Influencia de la Vegetación Urbana en la Calidad del Aire y Confort Climático (CGL2011-26173) funded by Spanish Ministry of Economy and Competitiveness.

References

- Krayenhoff, E.S., J.A. Voogt, 2007: A microscale three-dimensional urban energy balance model for studying surface temperatures. *Boundary-Layer Meteorology* **123**, 433-461.
- Santiago JL, Krayenhoff ES, Martilli A, 2014: Flow simulations for simplified urban configurations with microscale distributions of surface thermal forcing. *Urban Climate*. **9**, 115-133.
- Santiago JL, Martilli A, 2010: A dynamic urban canopy parameterization for mesoscale models based on computational fluid dynamics Reynolds-averaged Navier-Stokes microscale simulations. *Boundary-Layer Meteorology* **137**, 417-439.